Highly Stable Organic Antimony Halide Crystals for X-ray Scintillation

Qingquan He,[†] Chenkun Zhou,[‡] Liangjin Xu,[†] Sujin Lee,[†] Xinsong Lin,[†] Jennifer Neu,[§] Michael Worku,[⁋] Maya Chaaban,[†] and Biwu Ma*[,†,‡,⁋]

[†]Department of Chemistry and Biochemistry, Florida State University, Tallahassee, FL 32306, USA

[‡]Department of Chemical and Biomedical Engineering, FAMU-FSU College of Engineering, Tallahassee, FL 32310, USA

[§]National High Magnetic Field Laboratory, Florida State University, Tallahassee, Florida 32310, USA

[⁋]Materials Science and Engineering Program, Florida State University, Tallahassee, FL 32306, USA

ABSTRACT: Scintillators are utilized for X-ray detection in many important fields, from homeland security to health care. Developing low-cost high-performance scintillation materials to address the issues of existing commercially available ones is of great interest. Recently, organic metal halide hybrids have emerged as highly promising luminescent materials with excellent optical properties and low temperature solution processability. Herein, we report a zero-dimensional (0D) organic metal halide hybrid, $(PPN)_2SbCl_5$ (PPN = bis(triphenylphosphoranylidene)ammonium cation), as X-ray scintillation material with high light yield and exceptional environmental stability. Our study shows that $(PPN)_2SbCl_5$ single crystals prepared by solution growth exhibit visible photoluminescence with a quantum efficiency of 98.1 %. When excited by X-rays, $(PPN)_2SbCl_5$ single crystals exhibit radioluminescence with a near-perfect linearity in a large range of X-ray dose rate, and a comparable light yield (~ 49000 ph MeV^{-1}) with that of a commercial CsI(Tl) scintillator (~ 54000 ph MeV^{-1}). Moreover, the detection limit of $(PPN)_2SbCl_5$ (191.4 nGy_{air} s^{-1}) is much lower than the required value for regular medical diagnostics (5.5 μGy_{air} s^{-1}). $(PPN)_2SbCl_5$ single crystals also display remarkable stability with little-to-no change of properties after storage in ambient conditions for two years.

X-ray scintillators are scintillation-based indirect detectors, which absorb and down convert high-energy ionizing radiation into ultraviolet-visible light for detection of X-rays. As compared to direct X-ray detectors that convert X-ray to electric current, scintillators have numerous advantages, such as high response rate, large absorption cross section, and high stability.[1-5] Nowadays, scintillators are actively used in many important fields, including medical imaging,[6-8] non-invasive inspection,[9, 10] radiation monitoring,[5] and other industrial applications.[11, 12] Most of commercially available scintillators are based on inorganic single crystals, which are prepared *via* time-consuming high temperature processes in vacuum.[13, 14] To reduce the energy consumption for material preparation, many organic scintillators have been developed by low temperature processes, which however have inferior performance than inorganic ones with lower scintillation light yields and resolutions.[4] Developing scintillation materials by facile processes with high irradiation yield and sensitive remains a challenge.

Organic-inorganic metal halide perovskites and perovskite-related hybrids have recently emerged as highly promising materials for X-ray scintillation, owing to their characteristics of excellent luminescence properties, high absorption coefficients for ionizing radiation, and solution-process preparations.[15-26] For instance, methylammonium (MA) lead halide perovskite crystals, $MAPbI_3$ and $MAPbBr_3$, have displayed light yields of around 1000 photons per MeV (ph MeV^{-1}).[27] Liu and colleagues utilized all inorganic $CsPbBr_3$ nanocrystals to fabricate scintillating panels with good X-ray imaging.[2] Zhang et al. reported a light yield of 21000 ph MeV^{-1} for $CsPbBr_3$.[28] After that, Zeng and co-workers improved the stability and sensitivity of this kind of scintillator by employing $CsPbBr_3@Cs_4PbBr_6$, of which the light yield is still inferior to that of traditional scintillators.[5] Recently, Kishimoto et al. developed a perovskite-related hybrid scintillation material, phenethylamine lead bromide ($(PEA)_2PbBr_4$, which gave a light yield of 22 ± 2% of NaI(Tl) scintillator (~ 7600 ph MeV^{-1}).[29] Another organic lead halide hybrid $(EDBE)PbCl_4$ (EDBE = 2,2'-(ethylenedioxy)bis(ethylammonium)) was reported to have a light yield of ~ 9000 ph MeV^{-1} at room temperature.[27] While great potential has been shown in these materials, their real applications are still limited by the low long-term stability and lead toxicity.[30]

Lead-free low-dimensional metal halide hybrids have been developed to exhibit high luminescence and excellent stability, which make them highly attractive for X-ray scintillators.[29, 31-33] Recently, Tang and co-workers reported a lead-free 1D structure Rb_2CuBr_3 scintillator with a high light yield (~ 91000 ph MeV^{-1}) and good spectral stability of two months under ambient conditions.[30] A zero-dimensional (0D) $Bmpip_2SnBr_4$ (Bmpip = 1-butyl-1-methyl-piperidinium cation) based scintillator was reported by Kovalenko et al., to exhibit higher scintillation light yield than that of NaI(Tl).[34] However, the photoluminescence quantum efficiency (PLQE) of this material (75%) is still not optimal and the easy oxidation of Sn (II) to Sn (IV) leads to low stability. Therefore, developing highly stable luminescent 0D organic metal halide hybrids for scintillators with high light yield and stability upon X-ray irradiation is of great interest.

Here we report an X-ray scintillator based on 0D $(PPN)_2SbCl_5$ (PPN = bis(triphenylphosphoranylidene)ammonium) single crystals that can be prepared by a facile solution process at room temperature. $(PPN)_2SbCl_5$ single crystals exhibit dual-

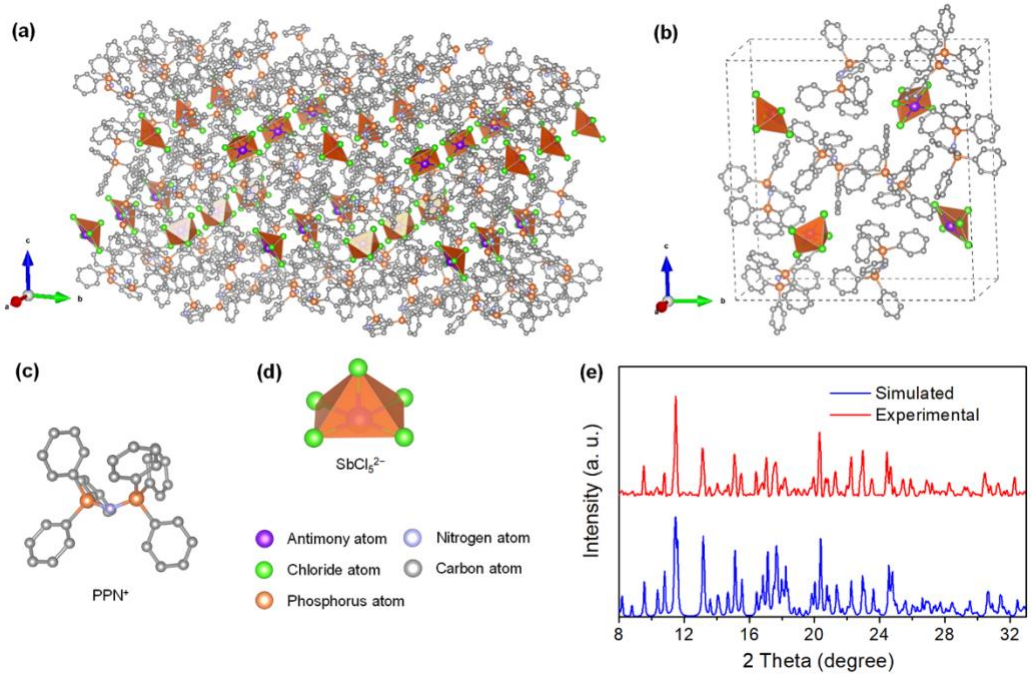

Figure 1. (a) View of single crystal structure of $(PPN)_2SbCl_5$ (hydrogen atoms were hidden for clarity). (b) Monoclinic unit cell of $(PPN)_2SbCl_5$. Structure of an individual (c) PPN^- cation and (d) $SbCl_5^{2-}$ anion. (e) Powder and simulated XRD patterns of $(PPN)_2SbCl_5$ single crystals.

band emission at UV excitation with a high PLQE of 98.1 %. The scintillation properties of $(PPN)_2SbCl_5$ were systematically investigated and revealed high radioluminescence (RL) intensity as well as low detection limit. $(PPN)_2SbCl_5$ single crystals also display remarkable stability in various conditions, such as continuous X-ray irradiation, high energy UV illumination, and storage in ambient conditions.

$(PPN)_2SbCl_5$ single crystals were prepared by injecting diethyl ether into dichloromethane precursor solution of $SbCl_3$ and PPNCl at room temperature in N_2-filled glovebox and stood for overnight. The detailed synthesis and characterization are presented in the Supporting Information. The crystal structure of the obtained $(PPN)_2SbCl_5$ single crystals was determined by single crystal X-ray diffraction (SCXRD) at 150 K. The results indicate that the isolated $SbCl_5^-$ anions ionically bonded to surrounding bulky PPN^+ cations, forming a typical 0D organic-inorganic metal halide hybrid structure with monoclinic $P2_1/c$ symmetry (Figure 1a-1c, Table S1). A single $SbCl_5^-$ anion clearly shows that each antimony atom is bonded to five chlorine atoms to form the pyramid structure (Figure 1d). The bond distance between Sb atom and apical Cl atom in $SbCl_5^{2-}$ anion is ~ 2.38 Å, while the lengths of the other Sb-Cl bonds are from 2.58 to 2.64 Å, which are comparable with reported $SbCl_5^{2-}$ structures (Table S2).[35-37] The powder XRD pattern of ground $(PPN)_2SbCl_5$ crystals is consistent with the simulated result based on its single crystal structure (Figure 1e), confirming the reliability of SCXRD measurement. This result also suggests the uniform of 0D crystals and the structure stability of single crystals at low temperature (150 K).

$(PPN)_2SbCl_5$ single crystals with size of several millimeters are light-yellow under ambient light (Figure S1a), and the corresponding band gap is calculated to be ~ 2.7 eV from UV-Vis spectrum (Figure S2). Under UV light irradiation (365 nm), the crystals display bright salmon pink luminescence with a high PLQE of 98.1 % (Figure S1b and S3). The photophysical

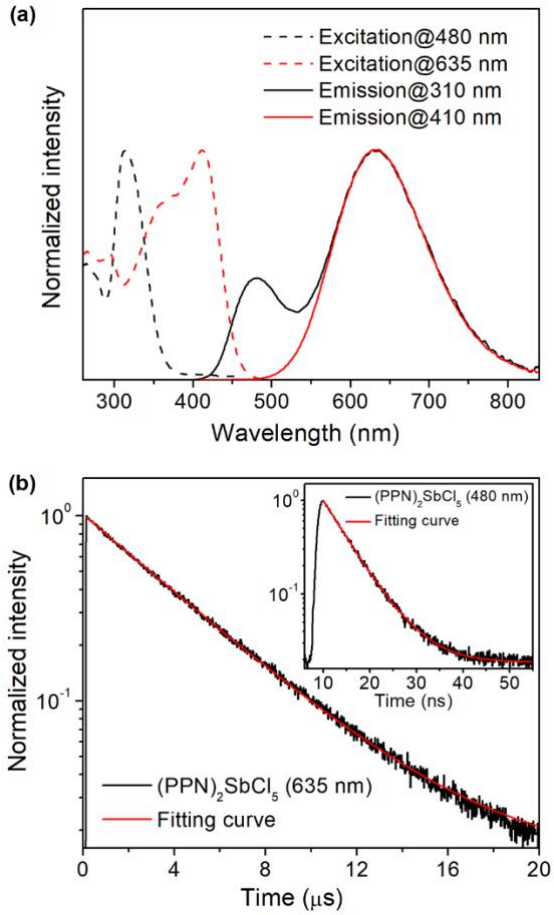

Figure 2. (a) Excitation and emission spectra of $(PPN)_2SbCl_5$ single crystals. (b) TRPL spectra of $(PPN)_2SbCl_5$ crystals at 635 nm and 480 nm (inset).

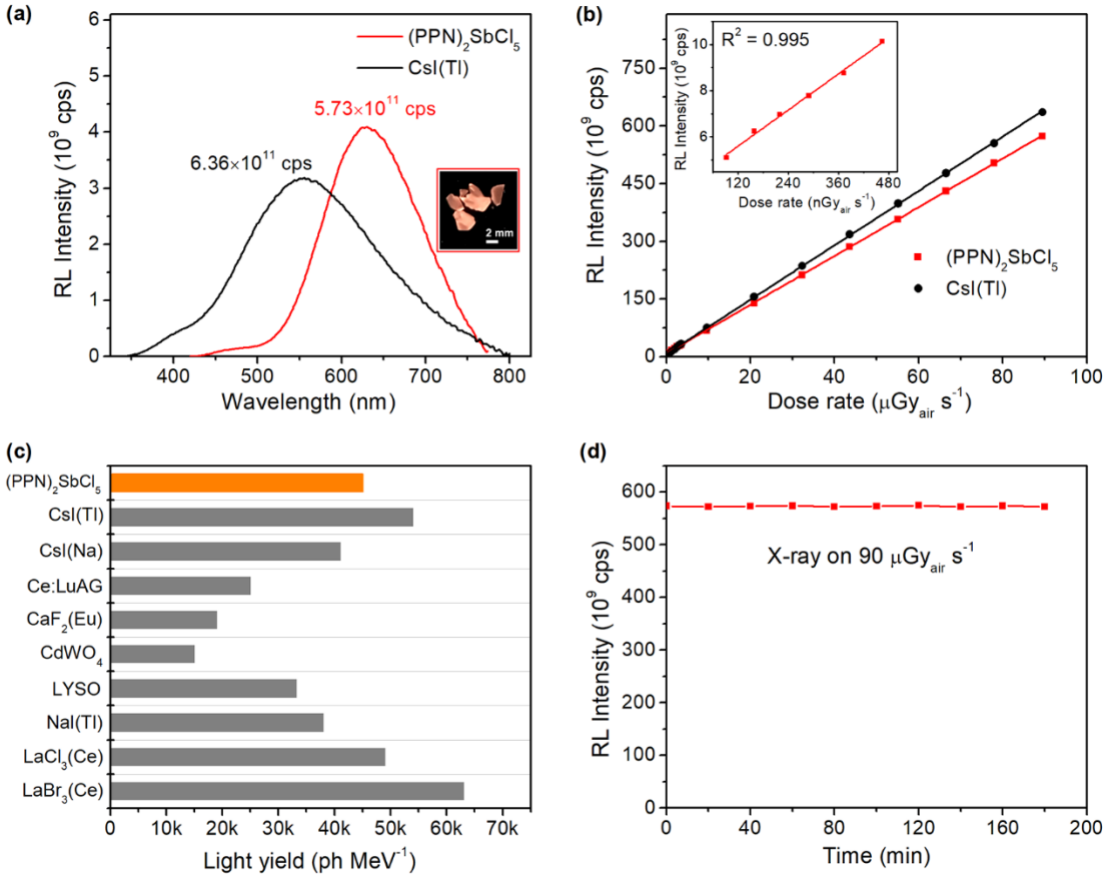

Figure 3. (a) RL spectra of $(PPN)_2SbCl_5$ and CsI(Tl) under 50 KeV of X-ray excitation. The inset is digital photograph of the $(PPN)_2SbCl_5$ crystals under X-ray irradiation. (b) Linear relationship between dose rate and RL intensity for $(PPN)_2SbCl_5$ and CsI(Tl) scintillators. The inset is the data of $(PPN)_2SbCl_5$ measured at low dose rate. (c) The comparison of scintillation light yields of $(PPN)_2SbCl_5$ and some commercial scintillators. (d) Stability of $(PPN)_2SbCl_5$ crystals against continuous X-ray irradiation.

properties of $(PPN)_2SbCl_5$ crystals were further investigated with steady photoluminescence (PL) and time-resolved PL (TRPL) spectra (Figure 2). PL spectra reveal that single crystals excited at 410 nm have a low-energy (LE) emission peaked at 635 nm with a large full width at half-maximum (FWHM) of 142 nm and a large Stokes shift of 225 nm (red curves in Figure 2a), and a long decay lifetime (τ_{LE}) of 4.1 μs (Figure 2b). This phosphorescent emission is believed to come from the radiative recombination of localized excitons in the inorganic $SbCl_5^{2-}$ pyramids that have pronounced excited state structural reorganization.[34-38] Such strongly Stokes shifted broadband emissions as a result of excited state structure reorganization have been observed in many previously reported Sn(II)-, Pb(II)-, and Sb(III)-based 0D organic metal halide hybrids.[3, 34, 35, 39, 40] The large Stokes shift is attributed to the pronounced excited state structural distortion in the excited state of $SbCl_5^{2-}$ pyramids upon photoactivation.[35, 39]

Interestingly, a new high-energy (HE) emission peak located at 480 nm was observed when the single crystals were excited at 310 nm (black curves in Figure 2b), which has a decay lifetime (τ_{HE}) of 5.4 ns (inset of Figure 2b), suggesting another emitting center that could possibly be the organic component.[41] To reveal the origin of this HE emission, PPNCl single crystals were prepared and measured to explore the luminescence of the organic component (Figure S5). The emission peaks of PPNCl appeared at around 480 nm, which is similar with the HE emission peak of $(PPN)_2SbCl_5$ (Figure S6), indicating that the organic component is likely responsible for HE emission. Meanwhile, the fluorescence emission from singlet localized excitons in $SbCl_5^{2-}$ pyramids was observed in this region as reported by Li et al.,[37] which might also attribute to the HE emission of $(PPN)_2SbCl_5$. Therefore, the HE emitting center could be assigned to intra-ligand charge transfer of organic cations PPN^+ and/or singlet localized excitons in $SbCl_5^{2-}$.[36, 37] Moreover, we also measured the PL spectra of $(PPN)_2SbCl_5$ crystals with excitation wavelengths varying from 280 to 380 nm and found that the intensity of high-energy emission peak enhanced firstly and then disappeared (Figure S4), resulting in excitation-dependent emission profiles.

Considering the high PLQE, the obtained 0D $(PPN)_2SbCl_5$ single crystals may be a candidate as scintillation material for X-ray radiation detection. Here, RL spectrum of $(PPN)_2SbCl_5$ was measured under 50 KeV X-ray excitation to investigate its scintillation performance (Figure 3a). A commercially available thallium activated cesium iodide (CsI(Tl)) scintillator was used as a reference to quantify the scintillation light yield of $(PPN)_2SbCl_5$. Under X-ray irradiation, $(PPN)_2SbCl_5$ single crystals exhibit similar spectrum with dual-band emission at ~ 480 and 635 nm as that of samples excited at 360 nm UV light (Figure S4), while CsI(Tl) also exhibit the same phenomenon (Figure S7), indicating the same radiative recombination channel under X-ray and UV excitations.[30] Importantly, although the absorption coefficient of $(PPN)_2SbCl_5$ is lower than that of CsI(Tl) due to the less existence of heavier elements (Figure S8), the count rate of $(PPN)_2SbCl_5$ (5.73×10^{11} cps) at the full energy peak is comparable to that of CsI(Tl) (6.36×10^{11}

cps), which can be attributed to its high quantum efficiency and little-to-no self-absorption.[28]

To further evaluate the scintillation performance, RL spectra of $(PPN)_2SbCl_5$ and CsI(Tl) scintillators under varied X-ray dose rates were measured by changing the power of X-ray tube (Figure S9). The RL intensities of both $(PPN)_2SbCl_5$ and CsI(Tl) are enhanced with the increasing of X-ray dose rate (Figure S10). Moreover, a linear relationship of X-ray dose rate versus RL intensity was recorded for $(PPN)_2SbCl_5$ in a large range from ~ 10 n Gy_{air} s^{-1} to 90 μGy_{air} s^{-1} (Figure 3b). The slope value of $(PPN)_2SbCl_5$ reaches ~ 91% of that of CsI(Tl). Thus, the light yield of $(PPN)_2SbCl_5$ can be estimated to be ~ 49000 ph MeV^{-1}, by referring to CsI(Tl) (54000 ph MeV^{-1}). The response of $(PPN)_2SbCl_5$ also displays a well linearity at the low range of X-ray dose rate (inset in Figure 3b), with a low detection limit of 191.4 nGy_{air} s^{-1}, which is much lower than the requirement for regular medical diagnostics (5.5 μGy_{air} s^{-1}).[17, 30, 42] By comparing with some other commercially available scintillators (Figure 3c), we found that the X-ray irradiation yield of $(PPN)_2SbCl_5$ is higher than or comparable with existing scintillators, indicating a desirable property for scintillation applications. The remarkable scintillation performance of $(PPN)_2SbCl_5$ can be attributed to its near-unity PLQE and large Stokes shift which resulted in high light yield and less self-absorption of luminescence, respectively.[27, 30]

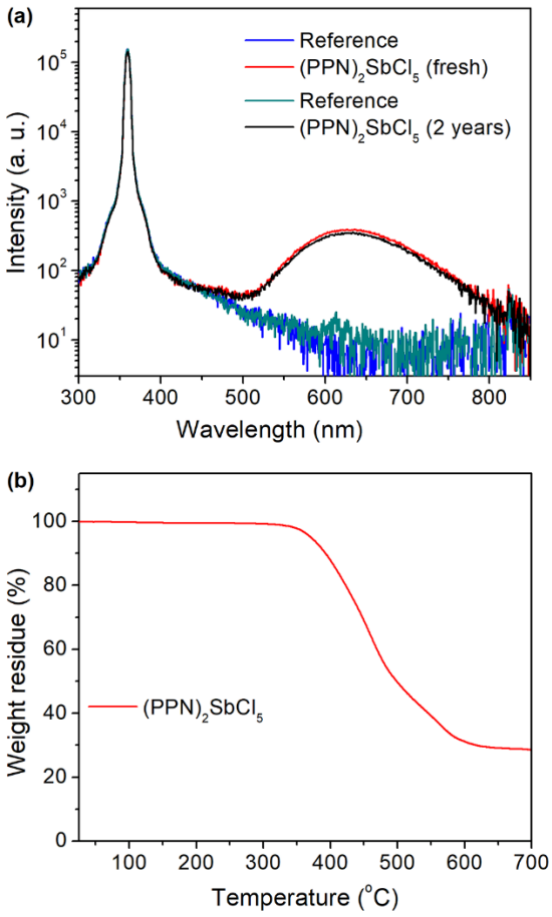

Figure 4. (a) Stability of $(PPN)_2SbCl_5$ crystals against long-term storage under ambient conditions. (b) TGA curve of $(PPN)_2SbCl_5$.

The stability of $(PPN)_2SbCl_5$ was characterized in various aspects. As shown in Figure 3d, $(PPN)_2SbCl_5$ has almost no light yield degradation upon continuous X-ray irradiation (90 μGy_{air} s^{-1}) for two hours. Under high-intensity UV illumination generated by a high-power mercury lamp (150 mW cm^{-2}) for two hours, the PL intensity of $(PPN)_2SbCl_5$ single crystals also remains unchanged (Figure S11). It is worth mentioning that $(PPN)_2SbCl_5$ also exhibits an excellent ambient stability. Single crystals could be kept in the solid state under ambient conditions with a relative humanity of 40 to 60% and temperature of around 25 ºC for two years with little-to-no change of PLQE (Figure 4a), i.e. the PLQE is 98.1 % for fresh $(PPN)_2SbCl_5$ and 97.4% for the same sample after two years' storage. The high stability of $(PPN)_2SbCl_5$ can be attributed to the formation of 0D crystal structure, in which bulky PPN^+ can dynamically stabilize the $SbCl_5^{2-}$ pyramids and protect them from outside environment.[32] The thermostability of $(PPN)_2SbCl_5$ crystals was characterized by employing thermogravimetric analysis (TGA in Figure 4b). The thermal decomposition temperature was measured at more than 300 °C, demonstrating high thermostability of $(PPN)_2SbCl_5$ single crystals. All these features suggest the great potential of practical application of this 0D organic metal halide hybrid.

In summary, we have developed a novel lead-free X-ray scintillation material, $(PPN)_2SbCl_5$, which can be prepared via a facile solution process to from single crystals with the size of several millimeters. This organic metal halide hybrid adapts a typical 0D structure at the molecular level, with isolated $SbCl_5^-$ anions ionically bonded to surrounding organic cations PPN^+. Optical spectroscopic studies show that $(PPN)_2SbCl_5$ has photo absorption in UV region and exhibits excitation dependent dual-band emissions from both organic and inorganic components. When excited with X-rays, the crystals display bright salmon pink luminescence and give high scintillation light yield of ~ 49000 ph MeV^{-1}. The response of $(PPN)_2SbCl_5$ scintillator displays a well linearity at a large range of X-ray dose rate and provides a low detection limit. Moreover, $(PPN)_2SbCl_5$ single crystals exhibit remarkable irradiation, storage, and thermal stabilities. Our work suggests a new way to develop low-cost eco-friendly high-performance X-ray scintillators.

ASSOCIATED CONTENT

Supporting Information

The Supporting Information is available free of charge on the ACS Publications website.

Experimental procedures, digital photographs, UV-Vis spectra, PLQE, excitation dependent spectra, and PL stability of $(PPN)_2SbCl_5$; Single crystal structure, excitation and emission spectra of PPNCl; Excitation and emission spectra of CsI(Tl); RL spectra of CsI(Tl) and $(PPN)_2SbCl_5$. Crystallographic information file of $(PPN)_2SbCl_5$.

[CCDC 1983725 contains the supplementary crystallographic data for this paper. These data can be obtained free of charge from The Cambridge Crystallographic Data Centre via www.ccdc.cam.ac.uk/data_request/cif.]

AUTHOR INFORMATION

Corresponding Author

*E-mail: bma@fsu.edu.

Notes

A U.S. Provisional Patent Application "X-ray Scintillators and Methods" has been filed by inventors Qingquan He, Liangjin Xu, and Biwu Ma.

ACKNOWLEDGMENT

The authors acknowledge the supports from the National Science Foundation (DMR-1709116), the Air Force Office of Scientific Research (AFOSR) (17RT0906), and the FSU Office of Research.

REFERENCES

1. Wang, Y. X.; Yin, X. M.; Liu, W.; Xie, J.; Chen, J. F.; Silver, M. A.; Sheng, D. P.; Chen, L. H.; Juan, D. W.; Liu, N.; Chai, Z. F.; Albrecht-Schmitt, T. E.; Wang, S. A., Emergence of Uranium as a Distinct Metal Center for Building Intrinsic X-ray Scintillators. *Angew. Chem. Int. Ed.* **2018,** *57*, 7883-7887.
2. Chen, Q. S.; Wu, J.; Ou, X. Y.; Huang, B. L.; Almutlaq, J.; Zhumekenov, A. A.; Guan, X. W.; Han, S. Y.; Liang, L. L.; Yi, Z. G.; Li, J.; Xie, X. J.; Wang, Y.; Li, Y.; Fan, D. Y.; Teh, D. B. L.; All, A. H.; Mohammed, O. F.; Bakr, O. M.; Wu, T.; Bettinelli, M.; Yang, H. H.; Huang, W.; Liu, X. G., All-inorganic perovskite nanocrystal scintillators. *Nature* **2018,** *561*, 88-93.
3. Tao, K. W.; Li, Y. B.; Ji, C. M.; Liu, X. T.; Wu, Z. Y.; Han, S. G.; Sun, Z. H.; Luo, J. H., A Lead-Free Hybrid Iodide with Quantitative Response to X-ray Radiation. *Chem. Mater.* **2019,** *31*, 5927-5932.
4. Maddalena, F.; Tjahjana, L.; Xie, A. Z.; Arramel; Zeng, S. W.; Wang, H.; Coquet, P.; Drozdowski, W.; Dujardin, C.; Dang, C.; Birowosuto, M. D., Inorganic, Organic, and Perovskite Halides with Nanotechnology for High-Light Yield X- and gamma-ray Scintillators. *Crystals* **2019,** *9*, 88.
5. Cao, F.; Yu, D.; Ma, W.; Xu, X.; Cai, B.; Yang, Y. M.; Liu, S.; He, L.; Ke, Y.; Lan, S.; Choy, K.-L.; Zeng, H., Shining Emitter in a Stable Host: Design of Halide Perovskite Scintillators for X-ray Imaging from Commercial Concept. *ACS Nano* **2019**, 10.1021/acsnano.9b06114.
6. El-Mohri, Y.; Antonuk, L. E.; Zhao, Q. H.; Wang, Y.; Li, Y. X.; Du, H.; Sawant, A., Performance of a high fill factor, indirect detection prototype flat-panel imager for mammography. *Med. Phys.* **2007,** *34*, 315-327.
7. Wei, H. T.; Huang, J. S., Halide lead perovskites for ionizing radiation detection. *Nat. Commun.* **2019,** *10*, 1066.
8. van Eijk, C. W. E., Inorganic scintillators in medical imaging. *Phys. Med. Biol.* **2002,** *47*, R85-R106.
9. Nikl, M.; Yoshikawa, A., Recent R&D Trends in Inorganic Single-Crystal Scintillator Materials for Radiation Detection. *Adv. Opt. Mater.* **2015,** *3*, 463-481.
10. Hanke, R.; Fuchs, T.; Uhlmann, N., X-ray based methods for non-destructive testing and material characterization. *Nucl. Instrum. Meth. A* **2008,** *591*, 14-18.
11. O'Nions, K.; Pitman, R.; Marsh, C., Science of nuclear warheads. *Nature* **2002,** *415*, 853-857.
12. Martin, T.; Koch, A.; Nikl, M., Scintillator materials for x-ray detectors and beam monitors. *Mrs Bull.* **2017,** *42*, 451-456.
13. Heo, J. H.; Shin, D. H.; Park, J. K.; Kim, D. H.; Lee, S. J.; Im, S. H., High-Performance Next-Generation Perovskite Nanocrystal Scintillator for Nondestructive X-Ray Imaging. *Adv. Mater.* **2018,** *30*, 1801743.
14. Liu, J. Y.; Shabbir, B.; Wang, C. J.; Wan, T.; Ou, Q. D.; Yu, P.; Tadich, A.; Jiao, X. C.; Chu, D. W.; Qi, D. C.; Li, D. B.; Kan, R. F.; Huang, Y. M.; Dong, Y. M.; Jasieniak, J.; Zhang, Y. P.; Bao, Q. L., Flexible, Printable Soft-X-Ray Detectors Based on All-Inorganic Perovskite Quantum Dots. *Adv. Mater.* **2019,** *31*, 1901644.
15. Li, Y.; Shao, W. Y.; Ouyang, X. P.; Zhu, Z. C.; Zhang, H.; Ouyang, X.; Liu, B.; Xu, Q., Scintillation Properties of Perovskite Single Crystals. *J. Phys. Chem. C* **2019,** *123*, 17449-17453.
16. Zhou, C. K.; Lin, H. R.; Neu, J.; Zhou, Y.; Chaaban, M.; Lee, S.; Worku, M.; Chen, B. H.; Clark, R.; Cheng, W. H.; Guan, J. J.; Djurovich, P.; Zhang, D. Z.; Lu, X. J.; Bullock, J.; Pak, C.; Shatruk, M.; Du, M. H.; Siegrist, T.; Ma, B. W., Green Emitting Single-Crystalline Bulk Assembly of Metal Halide Clusters with Near-Unity Photoluminescence Quantum Efficiency. *ACS Energy Lett.* **2019,** *4*, 1579-1583.
17. Wei, H. T.; Fang, Y. J.; Mulligan, P.; Chuirazzi, W.; Fang, H. H.; Wang, C. C.; Ecker, B. R.; Gao, Y. L.; Loi, M. A.; Cao, L.; Huang, J. S., Sensitive X-ray detectors made of methylammonium lead tribromide perovskite single crystals. *Nat. Photonics* **2016,** *10*, 333-339.
18. Gao, L.; Yan, Q. F., Recent Advances in Lead Halide Perovskites for Radiation Detectors. *Sol. RRL* **2019,** *4*, 1900210.
19. Mykhaylyk, V. B.; Kraus, H.; Saliba, M., Bright and fast scintillation of organolead perovskite $MAPbBr_3$ at low temperatures. *Mater. Horiz.* **2019,** *6*, 1740-1747.
20. Wang, L. L.; Fu, K. F.; Sun, R. J.; Lian, H. Q.; Hu, X.; Zhang, Y. H., Ultra-stable $CsPbBr_3$ Perovskite Nanosheets for X-Ray Imaging Screen. *Nano-Micro Lett.* **2019,** *11*, 52.
21. Hu, Q. S.; Deng, Z. Z.; Hu, M. C.; Zhao, A. J.; Zhang, Y. Q.; Tan, Z. F.; Niu, G. D.; Wu, H. D.; Tang, J., X-ray scintillation in lead-free double perovskite crystals. *Sci. China Chem.* **2018,** *61*, 1581-1586.
22. Li, L. Q.; Liu, X.; Zhang, H. J.; Zhang, B. B.; Jie, W. Q.; Sellin, P. J.; Hu, C. H.; Zeng, G. Q.; Xu, Y. D., Enhanced X-ray Sensitivity of $MAPbBr_3$ Detector by Tailoring the Interface-States Density. *ACS Appl. Mater. Interfaces* **2019,** *11*, 7522-7528.
23. Sun, Y.; Koshimizu, M.; Yahaba, N.; Nishikido, F.; Kishimoto, S.; Haruki, R.; Asai, K., High-energy X-ray detection by hafnium-doped organic-inorganic hybrid scintillators prepared by sol-gel method. *Appl. Phys. Lett.* **2014,** *104*, 174104.
24. Yahaba, N.; Koshimizu, M.; Sun, Y.; Yanagida, T.; Fujimoto, Y.; Haruki, R.; Nishikido, F.; Kishimoto, S.; Asai, K., X-ray detection capability of a Cs_2ZnCl_4 single-crystal scintillator. *Appl. Phys. Express* **2014,** *7*, 062602.
25. Kang, B.; Feng, Q. G.; Biswas, K., Comparative study of perovskite-type scintillator materials $CsCaI_3$ and $KCaI_3$ via first-principles calculations. *J. Phys. D: Appl. Phys.* **2018,** *51*, 065303.
26. Birowosuto, M. D.; Dorenbos, P., Novel gamma- and X-ray scintillator research: on the emission wavelength, light yield and time response of Ce^{3+} doped halide scintillators. *Phys. Status Solidi A* **2009,** *206*, 9-20.
27. Birowosuto, M. D.; Cortecchia, D.; Drozdowski, W.; Brylew, K.; Lachmanski, W.; Bruno, A.; Soci, C., X-ray Scintillation in Lead Halide Perovskite Crystals. *Sci. Rep.* **2016,** *6*, 37254.
28. Zhang, Y. H.; Sun, R. J.; Qi, X. Y.; Fu, K. F.; Chen, Q. S.; Ding, Y. C.; Xu, L. J.; Liu, L. M.; Han, Y.; Malko, A. V.; Liu, X. G.; Yang, H. H.; Bakr, O. M.; Liu, H.; Mohammed, O. F., Metal Halide Perovskite Nanosheet for X-ray High-Resolution Scintillation Imaging Screens. *ACS Nano* **2019,** *13*, 2520-2525.
29. Kishimoto, S.; Shibuya, K.; Nishikido, F.; Koshimizu, M.; Haruki, R.; Yoda, Y., Subnanosecond time-resolved x-ray measurements using an organic-inorganic perovskite scintillator. *Appl. Phys. Lett.* **2008,** *93*, 261901.
30. Yang, B.; Yin, L. X.; Niu, G. D.; Yuan, J. H.; Xue, K. H.; Tan, Z. F.; Miao, X. S.; Niu, M.; Du, X. Y.; Song, H. S.; Lifshitz, E.; Tang, J., Lead-Free Halide Rb_2CuBr_3 as Sensitive X-Ray Scintillator. *Adv. Mater.* **2019,** *31*, 1904711.
31. Shibuya, K.; Koshimizu, M.; Murakami, H.; Muroya, Y.; Katsumura, Y.; Asai, K., Development of ultra-fast semiconducting scintillators using quantum confinement effect. *Jpn. J. Appl. Phys.* **2004,** *43*, L1333-L1336.
32. Zhou, C.; Lin, H.; He, Q.; Xu, L.; Worku, M.; Chaaban, M.; Lee, S.; Shi, X.; Du, M.-H.; Ma, B., Low Dimensional Metal Halide Perovskites and Hybrids. *Mater. Sci. Eng. R Rep.* **2019,** *137*, 38-65.
33. Zhao, X.; Niu, G.; Zhu, J.; Yang, B.; Yuan, J.-H.; Li, S.; Gao, W.; Hu, Q.; Yin, L.; Xue, K.-H.; Lifshitz, E.; Miao, X.; Tang, J., All-Inorganic Copper Halide as a Stable and Self-Absorption-Free X-ray Scintillator. *J. Phys. Chem. Lett.* **2020,** *11*, 1873-1880.
34. Morad, V.; Shynkarenko, Y.; Yakunin, S.; Brumberg, A.; Schaller, R. D.; Kovalenko, M. V., Disphenoidal Zero-Dimensional Lead, Tin, and Germanium Halides: Highly Emissive Singlet and Triplet Self-Trapped Excitons and X-ray Scintillation. *J. Am. Chem. Soc.* **2019,** *141*, 9764-9768.
35. Zhou, C. K.; Worku, M.; Neu, J.; Lin, H. R.; Tian, Y.; Lee, S. J.; Zhou, Y.; Han, D.; Chen, S. Y.; Hao, A.; Djurovich, P. I.; Siegrist, T.; Du, M. H.; Ma, B. W., Facile Preparation of Light Emitting Organic Metal Halide Crystals with Near-Unity Quantum Efficiency. *Chem. Mater.* **2018,** *30*, 2374-2378.
36. Wang, Z. P.; Wang, J. Y.; Li, J. R.; Feng, M. L.; Zou, G. D.; Huang, X. Y., $[Bmim]_2SbCl_5$: a main group metal-containing ionic liquid exhibiting tunable photoluminescence and white-light emission. *Chem. Commun.* **2015,** *51*, 3094-3097.
37. Li, Z. Y.; Li, Y.; Liang, P.; Zhou, T. L.; Wang, L.; Xie, R. J., Dual-Band Luminescent Lead-Free Antimony Chloride Halides with Near-

Unity Photoluminescence Quantum Efficiency. *Chem. Mater.* **2019,** *31*, 9363-9371.
38. Han, D.; Shi, H.; Ming, W.; Zhou, C.; Ma, B.; Saparov, B.; Ma, Y.-Z.; Chen, S.; Du, M.-H., Unraveling luminescence mechanisms in zero-dimensional halide perovskites. *J. Mater. Chem. C* **2018,** *6*, 6398-6405.
39. Zhou, C. K.; Lin, H. R.; Tian, Y.; Yuan, Z.; Clark, R.; Chen, B. H.; van de Burgt, L. J.; Wang, J. C.; Zhou, Y.; Hanson, K.; Meisner, Q. J.; Neu, J.; Besara, T.; Siegrist, T.; Lambers, E.; Djurovich, P.; Ma, B. W., Luminescent zero-dimensional organic metal halide hybrids with near-unity quantum efficiency. *Chem. Sci.* **2018,** *9*, 586-593.
40. Lin, H.; Zhou, C.; Chaaban, M.; Xu, L.-J.; Zhou, Y.; Neu, J.; Worku, M.; Berkwits, E.; He, Q.; Lee, S.; Lin, X.; Siegrist, T.; Du, M.-H.; Ma, B., Bulk Assembly of Zero-Dimensional Organic Lead Bromide Hybrid with Efficient Blue Emission. *ACS Materials Lett.* **2019,** *1*, 594-598.
41. Yang, S. M.; Wu, D. B.; Gong, W. J.; Huang, Q. Q.; Zhen, H. Y.; Ling, Q. D.; Lin, Z. H., Highly efficient room-temperature phosphorescence and afterglow luminescence from common organic fluorophores in 2D hybrid perovskites. *Chem. Sci.* **2018,** *9*, 8975-8981.
42. Zhuang, R. Z.; Wang, X. J.; Ma, W. B.; Wu, Y. H.; Chen, X.; Tang, L. H.; Zhu, H. M.; Liu, J. Y.; Wu, L. L.; Zhou, W.; Liu, X.; Yang, Y., Highly sensitive X-ray detector made of layered perovskite-like $(NH_4)_3Bi_2I_9$ single crystal with anisotropic response. *Nat. Photonics* **2019,** *13*, 602-608.

Table of Contents